Desalination and Water Treatment
www.deswater.com

doi:10.5004/dwt.2019.23355

139 (2019) 319–326
January

Biomimetic prepared polyaniline/molybdenum disulfide nanosheet based electrochemical detection of bisphenol A

Jingyi Zhang[a], Qing Zhang[a], Nguyen Thi Oanh[a], Hongxia Qu[b], Huifang Xie[a,*], Jinming Kong[a,*]

[a]*Jiangsu Key Laboratory of Chemical Pollution Control and Resources Reuse, School of Environmental and Biological Engineering, email: 964703028@qq.com (J. Zhang), 1369447083@qq.com (Q. Zhang), 3458033684@qq.com (N.T. Oanh) Tel./Fax +86 25 84303109, email: huifangxie@njust.edu.cn (H. Xie), j.kong@njust.edu.cn (J. Kong)*
[b]*School of Chemical Engineering, Nanjing University of Science and Technology, Nanjing 210094, Jiangsu Province, China, email: qhx@njust.edu.cn (H. Qu)*

Received 27 February 2018; Accepted 24 October 2018

ABSTRACT

Biomimetic *in situ* hemin catalyzed polymerization of aniline was used to prepare several polyaniline (PANI) based nanocomposites and MoS_2/PANI composite was chosen to modify glassy carbon electrodes (GCE) because it showed the strongest electrochemical catalytic effect on bisphenol A (BPA). The electrochemical response of the modified GCE to BPA was investigated by differential pulse voltammetry (DPV). When the mass ratio of MoS_2 to aniline monomer was 0.036, the MoS_2/PANI/GCE had the highest peak currents, displaying remarkable synergistic effect for detection of BPA. The peak current was linear related to the concentration of BPA in the range from 0.001 to 0.1 μM and from 0.1 to 1 μM respectively. The modified electrode was successfully employed for the determination of BPA in leaching of commercial containers and satisfactory recoveries were obtained.

Keywords: Biomimetic polymerization; Polyaniline; Molybdenum disulfide; Differential pulse voltammetry; Determination of bisphenol A

1. Introduction

Monitoring trace contaminations is becoming more and more necessary to guarantee the human and environmental safety. So, novel sensitive, reliable and cost-effective detection methods and tools have been pursed [1]. Taking bisphenol A (BPA), a widely used and typical estrogenic-disrupting compound and posing serious threat to the living beings [2–5] as an example, some kinds of monitoring methods are reported including gas chromatography(GC) [6] and GC-mass spectrometry (GC-MS) [7], high performance liquid chromatography (HPLC) [8] and LC-MS [9], enzyme-linked immunosorbent assay (ELISA) [10], fluorescence immunosensor [11], biosensor[12,13] and so on. However, most of them require costly instrumentation and highly skilled users. Fortunately, electrochemical approaches supply the powerful candidates for detection of BPA [1,14].

The application of electrochemical analysis of BPA is limited by the passivation or fouling of electrode surface due to oxidation products [15–18]. Then a wide range of surface electrode modifiers, especially nanomaterials have been applied to make advancements including noble metal, metal oxide, carbon materials, polymers and composites [14,17,19,20]. MoS_2 is a well-defined layered material, in which the Mo atomic layer is clamped by two S layers, forming a sandwich structure via covalent bonding [21–23]. With the discovery of unprecedented physical, electronic, chemical, and optical properties, MoS_2 has attracted a significant amount of interests in electronics, optoelectronics, sensors, catalysis, gas separation, energy storage and conversion, water remediation, and biomedicine [22–29]. The nanometer scale spaces (NSSs) in the interlayer spacing of MoS_2 will beneficial to improve reaction conditions [25,30].

*Corresponding author.

However, bare MoS_2 appears to be agglomerated and stacking with decreasing the number of active sites [31,32] and low conductivity [23]. It can be good protocols to integrate MoS_2 with conductive polymer. For example, polypyrrole/MoS_2 and polyaniline (PANI)/MoS_2 were reported to have outstanding performance on supercapacitors [23,33]. Most recently, MoS_2/PANI showed increasing application potential in the fields of lithium-ion batteries [34,35], photocatalysis [36] and fabrication of electrodes [16,37–39].

Our previous work provided an eco-friendly and simple method of preparation of PANI composites through in situ hemin catalyzed polymerization of aniline [40,41]. Hemin is a natural metallporphyrin and the active center of the heme-protein family with the properties of peroxidase. Hemin/MoS_2 exhibit enhanced peroxidase-like activity [42]. On the basis of the aforementioned works, we thought that MoS_2 nanosheet could be used to composite with PANI polymerized with biomimetic process. The properties and application on modifying electrodes of as-synthesized MoS_2/PANI have not been investigated before.

Herein, MoS_2/PANI and other several PANI-based composites were prepared using in situ hemin catalyzed polymerization. After comparing their ability to improve the properties of glass carbon electrodes (GCE), the MoS_2/PANI/GCE was screened as the sensing platform for sensitive detection of BPA. Our results indicated that this MoS_2/PANI/GCE exhibited high sensitivity, good reproducibility and long-term stability. The eco-friendly and simple sensor proved to be promising tool for detection of BPA.

2. Experimental

2.1. Apparatus and reagents

Electrochemical measurements were performed on a CHI660D electrochemical workstation (CH Instruments, China) with a three-electrode system. A saturated calomel electrode and a platinum wire were used as reference electrode and counter electrode respectively, and glassy carbon electrode (GCE) or fabricated GCE was used as working electrode. The ultrasonic process was performed with a KF-C sonifier (KenfenElectronic Technology, China.). Scanning electron microscopy (SEM, JSM-6700F, JEOL, Japan) and X ray diffraction (XRD, Bruker D8 Advance, Germany) were used to characterize the prepared composites. TGA curves were recorded on a TGA/SDTA 851e diffractometer.

Hemin (Bioduly, Co. Ltd, Nanjing China) is biological reagent and all other reagents are of analytical grade. MoS_2 was purchased from Shandong West Asia Chemical Industry Co., Ltd, China. BPA stock solution was prepared with ultrapure water and diluted to a certain concentration with pH = 7.0 phosphate buffer solution (PBS).

2.2. Preparation of PANI-based nanocomposite

A certain amount of metal oxides or sulfides was dispersed in 100 mL 0.1 M pH 4.0 citrate buffer solution by sonication for 4 h. Then a certain concentration hemin and 0.5 g aniline were added. The polymerization process of aniline were carried out according to our previous report. The composites of Fe_3O_4/PANI, ZnO/PANI, CuO/PANI, MoS_2/PANI and CdS/PANI were prepared for the future use.

2.3. Electrode preparation and fabrication

The GCE was polished with 0.3 μm alumina to get a smooth surface, and washed sequentially with, anhydrous alcohol under sonication. For each kind of the as-prepared composite, 0.5 mg was dispersed in 1 mL ultrapure water by sonication for 1 h. Then a 20 μL aliquot of the composite solution was applied to the polished GCE and left dry naturally in the air at room temperature.

2.4. Electrochemical measurements

Different concentrations of BPA were measured by differential pulse voltammetry (DPV) in the range of –1.0~1.0 V and the pulse amplitude, pulse width and pulse period were 0.05 V, 0.06 s and 0.2 s, respectively. PBS (pH 7.0) was used as supporting electrolyte. Electrochemical impedance spectroscopy (EIS) measurements were carried out in 5.0 mM $[Fe(CN)_6]^{3-/4-}$ solution containing 0.1 M KCl, with the frequencies swept from10 mHz to 100 kHz. The applied perturbation amplitude was 5 mV. Cyclic voltammogram (CV) measurements were applied from –0.8 to 0.8 V in pH = 7.0 PBS containing 1.0×10^{-6} M BPA at the scan rate of 100 mV s^{-1}.

3. Results and discussion

3.1 Comparison of PANI-based composites

Three kinds of metal oxides (Fe_3O_4 nanoparticle, ZnO and CuO) and two kinds of sulfides (MoS_2 and CdS) were chosen to prepare the PANI-based composites and to modify the electrode. The DPV profiles of 1.0×10^{-6} M BPA at different fabricated GCE in PBS (pH 7.0) are shown in Fig. 1.

Compared to PANI/GCE, the five modified GCE with PANI-based composites all showed higher oxidation peak currents and the MoS_2/PANI/GCE had the highest of response value. Results show the metal oxides and sulfide can enhance the electrochemical oxidation of BPA and MoS_2 renders the remarkable synergistic effects with PANI. MoS_2 is a kind of nanomaterial with two-di-

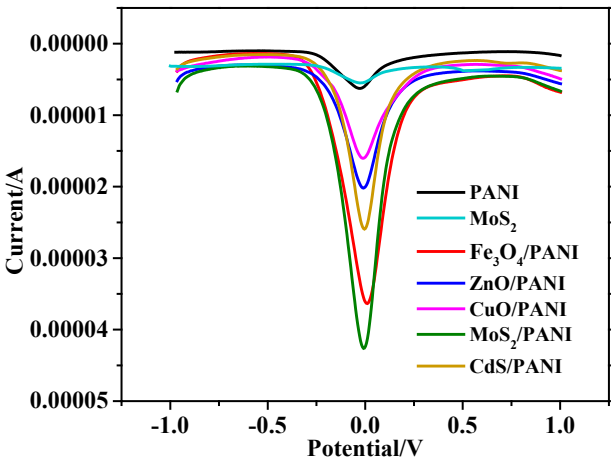

Fig. 1. DPVs of BPA with electrodes fabricated by different PANI-based composites.

mensional layers and showed unique electronic properties [22], maybe it is the reason for enhancement of signals. So, MoS_2/PANI is screened as the fabricating composite for the detail search.

3.2. Characterization of MoS_2/PANI composites

The morphologies of MoS_2, PANI and MoS_2/PANI were characterized by SEM and images are shown in Fig. 2.

MoS_2 presents the thin-layered structure with smooth surface and biomimetic prepared PANI is the irregular fine particles with diameter about 0.3~3.5 μm. The surface of MoS_2 is negatively charged at pH 1.5–10.5 [27], and the amine groups are easily protonated and positively charged [27,43], so PANI is easily coated on MoS_2 due to electrostatic attraction. The SEM image of MoS_2/PANI proves that the two shapes of materials are interwoven and randomly oriented in the composite. The fine diameter of composite indicates it had a large specific surface area [37,44]. The irregular structure and random alignment of MoS_2/PANI composite are benefit for the adsorption of BPA on the surface. On the other hand, the irregular structure can also result in a less compact film of oxidation products, which is the main reason of low sensitivity of bare GCE. Ghanam et al. [18] found that the suitable particle size and specific surface area can reduce significantly the fouling problem. The similar anti-fouling ability was also observed on the GCE fabricated by carbon nanotube due to the irregular structure and random alignments [15].

As can be seen in Fig. 3, the XRD spectra of MoS_2/PANI contains the characteristic peaks of MoS_2 (2θ = 14.4°, 32.7°, 33.5°, 35.9°, 39.6°, 49.8°, 58.4°, 60.4°) and PANI (2θ = 14.8°, 19.8° and 25.7°), which indicate that there is a combination between PANI and MoS_2 [23,27]. Meanwhile, the intensity of MoS_2 peaks decrease dramatically may be due to the PANI coating. In a word, PANI grows and partly coats on thin-layered MoS_2 with a compact combination in the MoS_2/PANI composite.

The TGA measurement was carried out to compare the thermal stability of PANI, MoS_2 and MoS_2/PANI. The initial mass loss around 100°C for three materials was attributed to the evaporation of surface absorbed water. MoS_2 nanosheet lost only 9.8% of its weight until 800°C. The TGA curves for PANI shows a two-step weight loss because of the elimination of the doped acid bound to PANI chains (200~350°C) and decomposition of the pristine PANI backbone (>350°C), respectively [45,46]. The weight loss of MoS_2/PANI was more than that of PANI under 342°C, which may be attributed to the loss of co-intercalated water, HCl and hemin in the NSSs. However, the mass loss is much lower at the higher temperature (>342°C) in comparison to that of PANI. The results indicated that the MoS_2/PANI composites has been successfully prepared.

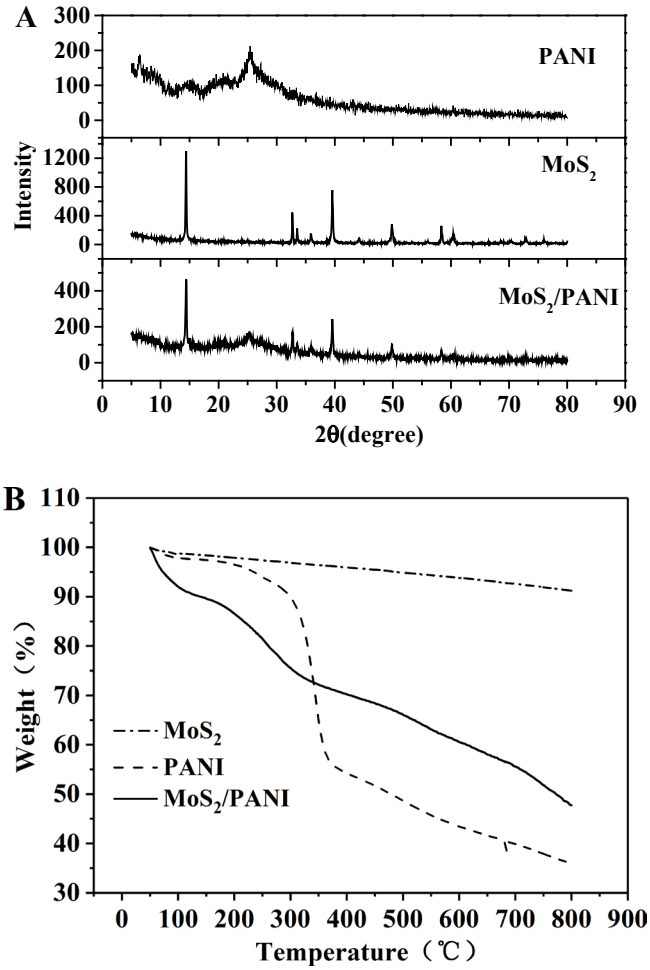

Fig. 3. XRD spectra (A) and TGA (B) of PANI, MoS_2 and MoS_2/PANI.

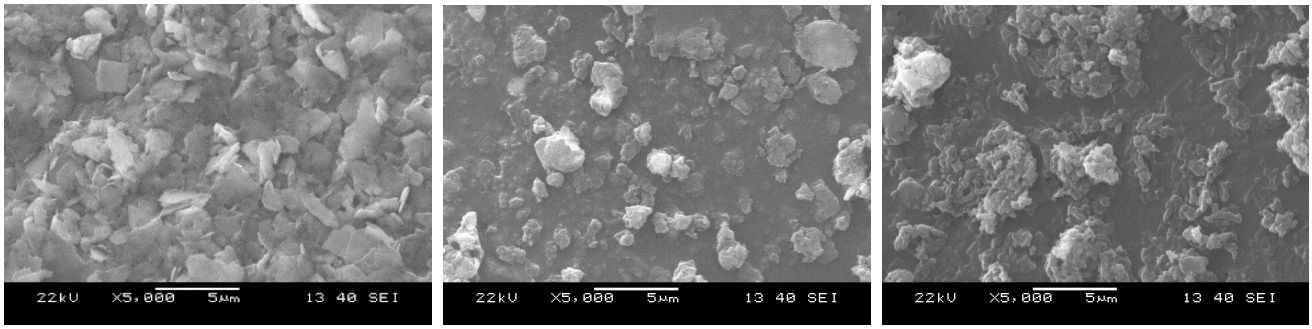

MoS_2 PANI MoS_2/PANI

Fig. 2. SEM images of (a) MoS_2, (b) PANI and (c) MoS_2/PANI.

3.3. Electrochemical properties of different electrodes

EIS can provide information on the impedance changes of the electrode surface during the modification process. At high frequency, the semicircular part corresponds to the electron transfer-limited process, and the diameter is equivalent to the Rct at electrode surface [47].

As shown in Fig. 4, the interfacial electron transfer resistance of the bare electrode was large (curve a). When the electrode was modified with MoS_2 (curve b), the value of Rct increased, indicating that MoS_2/GCE has poor conductivity [48]. After modification with PANI (curve c), the diameter of the high-frequency semicircle was very small, which may be ascribed to the existence of conductive polymer and its large specific surface area [23,43]. Finally, MoS_2/PANI/GCE (curve d) was tested and similar semicircle was noted, but the Rct of MoS_2/PANI/GCE was bigger than that of PANI/GCE. This also indicated that MoS_2 and PANI were successfully immobilized onto the surface of GCE.

3.4. Electrochemical behaviors of BPA

The electrochemical behaviors of BPA at the bare and the modified electrodes were investigated by CV in 0.1 M PBS (pH 7.0) containing 1.0×10^{-6} M BPA and the results are shown in Fig. 5.

At bare GCE (curve a), no redox peaks were observed, which is consistent with previous reports [49,50]. When the electrode was modified with MoS_2 (curve b), there were also no redox peaks, which may be attributed to the poor conductivity of MoS_2 [50]. At PANI/GCE, a couple of redox peaks were found (curve c), with a peak potential difference (ΔEp) of 0.3 V, indicating that PANI had higher electron transfer rate and electrical conductivity compared to GCE and MoS_2. After modifying the electrode with PANI/MoS_2, a significant increase in peak current was observed and the ΔEp was smaller (approximately 0.2 V). The peak current intensity at MoS_2/PANI /GCE was approximately 2-fold higher than that at PANI/GCE. The remarkable peak current enhancement may be attributed to the enlarged specific surface area of the electrode after modification and the synergistic effect of PANI and MoS_2. A similar behaviour has been observed in previous reports for oxidation of BPA [3,49].

3.5. Effects of MoS_2 content on the detection of BPA

In order to investigate the effects of MoS_2 content on the detection of BPA, different composites were prepared by adding different quantity of MoS_2 (18 mg, 36 mg, 54 mg and 72 mg) in the polymerization of 1.0 g aniline and were denoted as MoS_2 (18 mg)/PANI, MoS_2 (36 mg)/PANI, MoS_2 (54 mg)/PANI and MoS_2 (72 mg)/PANI respectively. The DPVs of 1.0×10^{-6} M BPA on PANI, MoS_2 and the fabricated electrodes by those different MoS_2/PANI are shown in Fig. 6.

As shown in Fig. 6, MoS_2 has weak electrocatalytic activity for BPA, it may due to the low conductivity. PANI/

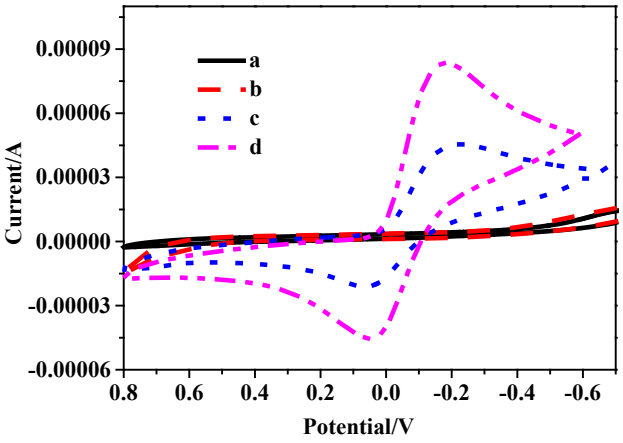

Fig. 5. CVs of different electrodes: (a) GCE, (b) MoS_2/GCE, (c) PANI/GCE and (d) MoS_2/PANI/GCEin the phosphate buffer solution buffer (pH 7.0) containing 1.0×10^{-6} M BPA. Scan rate: 100 mV s^{-1}.

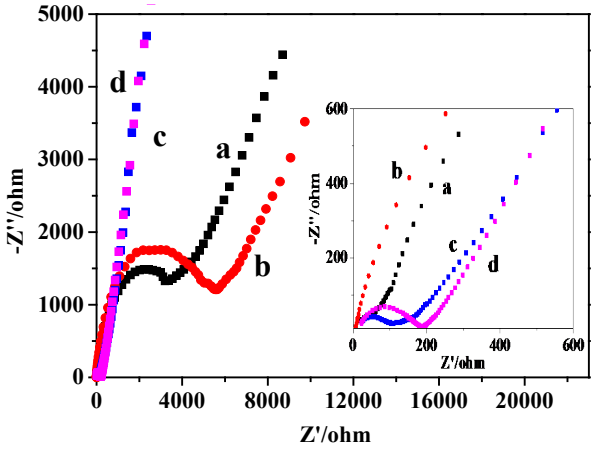

Fig. 4. EIS of (a) GCE, (b) MoS_2/GCE, (c) PANI/GCE and (d) MoS_2/PANI/GCE in 5 mM $[Fe(CN)_6]^{3-/4-}$ solution containing 0.1 M KCl. Inset is the magnified plots of (a), (b), (c) and (d) at the high-frequency region.

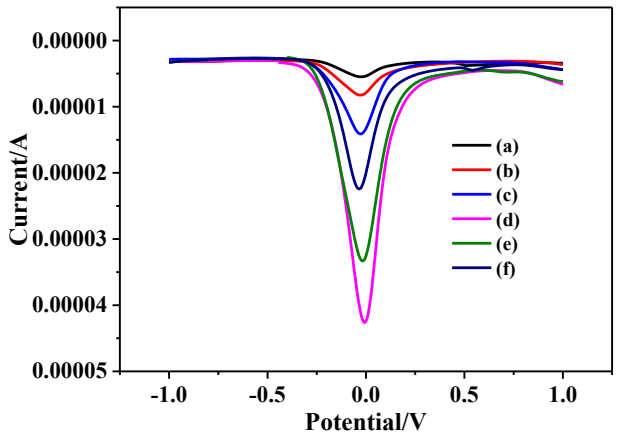

Fig. 6. DPVs of 1.0×10^{-6} M BPA at (a) MoS_2/GCE, (b) PANI/GCE, (c) MoS_2 (18 mg)/PANI/GCE, (d) MoS_2 (36 mg)/PANI/GCE, (e) MoS_2 (54 mg)/PANI/GCE and (f) MoS_2 (72 mg)/PANI/GCE.

GCE has a little higher current signal. Comparing the two response values of PANI/GCE or MoS_2/GCE, the electrochemical signals of the MoS_2/PANI composite are obviously larger. The largest current response occurred on the MoS_2 (36 mg)/PANI/GCE (curve d) and decreased with the increase of MoS_2 content. Thus, MoS_2 (36 mg)/PANI was chosen as the fabricating materials.

The electrocatalysis of nanomaterial relies on its defects, large exposed active edge site and excellent conductivity [22]. Bare MoS_2 appears to be agglomerated and stacking with decreasing the number of active sites [31,32] and low conductivity. The inducement of conductive PANI is very helpful to overcome the problem. The suitable ratio of MoS_2 to aniline during the polymerization makes the partial coat of PANI on the thin-layered MoS_2, thus effectively prevent accumulation, stack of MoS_2 and improve the electron transfer. More MoS_2 in the composite decrease the signals may be due to the decreasing active sites because of the accumulation and stack of MoS_2.

On the other hand, MoS_2/PANI has strong affinities and good adsorption capacity to the phenolic estrogenic compounds due to the π-π and electrostatic interaction [39]. Our adsorption experiments showed that the adsorption capacity of MoS_2/PANI for BPA can reach 17 mg/g (data not shown). The effective adsorption lays the foundation for the electrochemical reaction of BPA.

As a result, the electron exchange between BPA and the electrode surface is facilitated and further provides an excellent platform for BPA detection.

3.6. Analytical performance of MoS_2/PANI/GCE

A series of concentration of BPA was detected at MoS_2 (36 mg)/PANI/GCE by DPV and the results are displayed in Fig. 7.

As shown in Fig. 7a, it is apparent that the intensity of peak current increases with the increase of BPA concentration. According to the calibration plots of the peak current (I_p, μA) versus different concentrations of BPA (C, μM), two line segments can be seen. In the high concentrations range (0.1–1.0 μM), the linear relationship is I_p = 30.0986 C + 9.1854 (R^2 = 0.9923) and in the low concentrations range (0.001 – 0.1 μM), it is I_p = 98.0624C + 3.0032 (R^2 = 0.9979). The detection limit was estimated to be 4.9 nM (3σ).

The analytical performance of this fabricated electrode was compared with some of recently reported modified GCEs for BPA detection by DPV in Table 1. Compared to these reported modified GCE, it can be seen that MoS_2/PANI/GCE had relatively low detection limit and a wide linear range. The low detection limit could be related to the synergistic effects of the large surface area and the excellent conductivity of MoS_2 and PANI. Thus, the proposed sensor may be a better platform for the determination of BPA.

The relative standard deviation was 4.82% when ten MoS_2 (0.036 g)/PANI/GCEs were prepared and used to detect 1.0×10^{-6} M BPA at same conditions, which indicating a good reproducibility for detection of BPA.

After the fabricated electrode was stored for 2 weeks at room temperature, the peak current of detecting 1.0×10^{-6} M BPA was about 92% of the initial value, displaying its good stability.

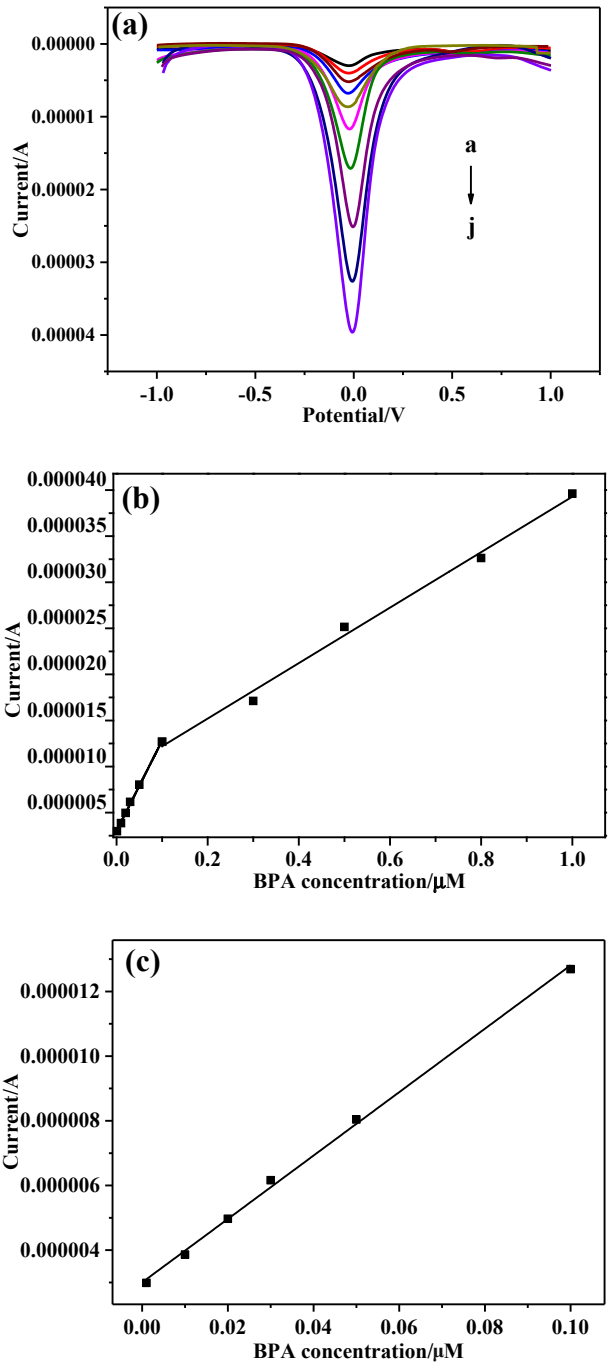

Fig. 7. (a) DPVs of a series of concentrations of BPA at MoS_2 (36 mg)/PANI/GCE in PBS (a–j, 0.001, 0.01, 0.02,0.03,0.05, 0.1, 0.3, 0.5, 0.8, 1.0 μM). (b) Calibration plots of the peak current versus different concentrations of BPA. (c) Low concentration partial enlargement of figure (b).

3.7 Detection of real samples

Possible migration of BPA into water from polyethylene terephthalate (PET) water bottle and disposable paper cup under severe conditions are investigated in this study. PBS (pH 7.0, 100 mL) was put into the container and it was placed in the microwave oven for 10 min at 700 W. After cooling to

Table 1
Comparison of the proposed method with some recently reported modified GCEs for BPA detection by DPV

Modifers of GCE	Linear range/ μM	Detection limit/nM	Reference
ELDH	0.02–1.51	6.8	[51]
AuNP/MWCNT	0.01–0.07	4	[52]
Fe_3O_4NPs-Si4Pic$^+$Cl$^-$/ Au NPs-Si4Pic$^+$Cl$^-$	0.02–1.40	7.0	[53]
AuPdNPs/GNs	0.05–10	8	[54]
ILs-LDH	0.02–3	4.6	[55]
MIPPy/GQDs	0.1–50	40	[56]
MIPs-AB	0.005–0.20, 0.50–10.00	2	[57]
MWCNTs-PEI	0.01–50	3.3	[58]
MoS_2-SPAN	0.001–1.0	0.6	[16]
PGA/MWCNT-NH_2	0.1–10	20	[59]
CS/MNPs-rGO	0.06–11	16.7	[60]
MoS_2/PANI	0.001–0.1, 0.1–1.0	4.9	This work

ELDH: Exfoliated Ni_2Al-layered double hydroxide nanosheets; AuNP/MWCNT: Multiwalled carbon nanotube and gold nanoparticle; Fe_3O_4 NPs-Si4Pic$^+$Cl$^-$/Au NPs-Si_4Pic$^+$Cl$^-$: A film of ferroferric oxide nanoparticles over a film of gold nanoparticles, both stabilized in a polymer solution of 3-n-propyl-4-picolinium silsesquioxane chloride; AuPdNPs/GNs: AuPd nanoparticles/ graphene composites; ILs-LDH: Ionic liquid functionalized Zn-Al layered double hydroxide; MIPPy/GQDs: Molecularly imprinted polypyrrole/graphene quantum dots composite; MIPs-AB: Molecularly imprinted chitosan film doping with acetylene black; MWCNTs-PEI: multi-walled nanotubes-polyethylenimine composites; MoS_2-SPAN: MoS_2 intercalated into self-doped PANI; PGA/MWCNT-NH_2: Polyglutamic acid/ amino-functionalised carbon nanotubes nanocomposite; CS/ MNPs-rGO: Chitosan/magnetic nanoparticles decorated reduced grapheme oxide.

Table 2
Determination of BPA in real samples using MoS_2/PANI/GCE (n = 3)

Samples	Spiked/ μM	Founded/ μM	RSD (%)	Recovery (%)
PET water bottle	0	0.002	7.6	
	0.200	0.206	2.9	102.0
Disposable paper cup	0	0.096	5.3	
	0.200	0.315	2.4	106.4

room temperature, the water sample directly detected using MoS_2/PANI/GCE by DPV. The standard addition method was carried out to evaluate the analytical performance. The results are shown in Table 2. The RSD in the range of 2.4–7.6% and the recoveries are 102.0% and 106.4% respectively, which proved that the MoS_2/PANI/GCE can be used to detect BPA in the practical water samples.

4. Conclusion

Among the composites prepared through in situ hemin catalyzed polymerization of aniline, MoS_2/PANI composite was chosen because it showed the strong electrochemical catalytic effect on BPA at the fabricated GCE. When the mass ratio of MoS_2 to aniline monomer was 0.036, the MoS_2/PANI/GCE has the highest peak currents, displaying the remarkable synergistic effect for detection of BPA. The detection of BPA at MoS_2/PANI/GCE displayed high response values, wide linear range, low detection limit and acceptable reproducibility and stability. The biomimetic preparation of MoS_2/PANI composite provides a simple and eco-friendly method for constructing electrode. Such biomimetic synthesizing strategy can be further extended to prepare the composites based on MoS_2 and other conductive polymers. Besides, the MoS_2/PANI composite electrode has potential application for detecting other phenolic estrogenic compounds or the substitute for bisphenol A, which are studied in detail in our lab.

Acknowledgments

This work was supported by the National Natural Science Foundation of China (grant numbers 21575066 and 51778296).

References

[1] M. Díaz-González, M. Gutiérrez-Capitán, P. Niu, A. Baldi, C. Jiménez-Jorquera, C. Fernández-Sánchez, Electrochemical devices for the detection of priority pollutants listed in the EU water framework directive, TrAC, Trends Anal. Chem., 77 (2016) 186–202.
[2] Y. Liu, X. Dong, P. Chen, Biological and chemical sensors based on graphene materials, Chem. Soc. Rev., 41 (2012) 2283–2307.
[3] X. Niu, W. Yang, G. Wang, J. Ren, H. Guo, J. Gao, A novel electrochemical sensor of bisphenol A based on stacked graphene nanofibers/gold nanoparticles composite modified glassy carbon electrode, Electrochim. Acta, 98 (2013) 167–175.
[4] N. Benachour, A. Aris, Toxic effects of low doses of bisphenol-A on human placental cells, Toxicol. Appl. Pharmacol., 241 (2009) 322–328.
[5] M.H. Dehghani, E. Nikfar, A. Zarei, N.M. Esfahani, The effects of US/H_2O_2 process on bisphenol-A toxicity in aqueous solutions using Daphnia magna, Desal. Water Treat., 68 (2017) 183–189.
[6] H.S. Shin, C.H. Park, S.J. Park, H. Pyo, Sensitive determination of bisphenol A in environmental water by gas chromatography with nitrogen-phosphorus detection after cyanomethylation, J. Chromatogr. A, 912 (2001) 119–125.
[7] S.C. Cunha, A. Pena, J.O. Fernandes, Dispersive liquid-liquid microextraction followed by microwave-assisted silylation and gas chromatography-mass spectrometry analysis for simultaneous trace quantification of bisphenol A and 13 ultraviolet filters in wastewaters, J. Chromatogr. A, 1414 (2015) 10–21.
[8] A. Cydzik-Kwiatkowska, K. Bernat, M. Zielińska, K. Bułkowska, I. Wojnowska-Baryła, Aerobic granular sludge for bisphenol A (BPA) removal from wastewater, Int. Biodeterior. Biodegrad., 122 (2017) 1–11.
[9] C. Postigo, M. Kuster, M. Villagrasa, S. Rodríguez-Mozaz, R. Brix, M.L. Farré, M.L.D. Alda, D. Barceló, Liquid chromatography—mass spectrometry methods for analysis of endocrine-disrupting chemicals in wastewaters, Springer Berlin Heidelberg, Berlin, Heidelberg, 2009, pp. 227–271.

[10] M.J. Moreno, P. D'Arienzo, J.J. Manclús, A. Montoya, Development of monoclonal antibody-based immunoassays for the analysis of bisphenol A in canned vegetables, J. Environ. Sci. Health., Part B, 46 (2011) 509–517.
[11] S. Rodriguez-Mozaz, M.L.D. Alda, D. Barcelo, Analysis of bisphenol A in natural waters by means of an optical immunosensor, Water Res., 39 (2005) 5071–5079.
[12] Y.X. Chen, K.J. Huang, K.X. Niu, Recent advances in signal amplification strategy based on oligonucleotide and nanomaterials for microRNA detection-a review, Biosens. Bioelectron., 99 (2017) 612–624.
[13] Y.X. Chen, K.J. Huang, L.L. He, Y.H. Wang, Tetrahedral DNA probe coupling with hybridization chain reaction for competitive thrombin aptasensor, Biosens. Bioelectron., 100 (2017) 274.
[14] K.V. Ragavan, N.K. Rastogi, M.S. Thakur, Sensors and biosensors for analysis of bisphenol-A, TrAC, Trends Anal. Chem., 52 (2013) 248–260.
[15] X. Liu, H. Feng, Electrocatalytic detection of phenolic estrogenic compounds at NiTPPS|carbon nanotube composite electrodes, Anal. Chim. Acta, 689 (2011) 212–218.
[16] T. Yang, H. Chen, R. Yang, Y. Jiang, W. Li, K. Jiao, A glassy carbon electrode modified with a nanocomposite consisting of molybdenum disulfide intercalated into self-doped polyaniline for the detection of bisphenol A, Mikrochim. Acta, 182 (2015) 2623–2628.
[17] S.H. Liang, C.C. Fong, X. Zhang, L.L. Chan, K.S. Lam, P.K. Chu, K.Y. Wong, M. Yang, Au nanoparticles decorated TiO_2 nanotube arrays as a recyclable sensor for photo-enhanced electrochemical detection of bisphenol A, Environ. Sci. Technol., 50 (2016) 4430.
[18] A. Ghanam, A.A. Lahcen, A. Amine, Electroanalytical determination of bisphenol A: investigation of electrode surface fouling using various carbon materials, J. Electroanal. Chem., 789 (2017) 58–66.
[19] G. Maduraiveeran, W. Jin, Nanomaterials based electrochemical sensor and biosensor platforms for environmental applications, Trends Environ. Anal. Chem., 13 (2017) 10–23.
[20] K.J. Huang, Y.J. Liu, Y.M. Liu, L.L. Wang, Molybdenum disulfide nanoflower-chitosan-Au nanoparticles composites based electrochemical sensing platform for bisphenol A determination, J. Hazard. Mater., 276 (2014) 207–215.
[21] X. Wang, J. Ding, S. Yao, X. Wu, Q. Feng, Z. Wang, B. Geng, High supercapacitor and adsorption behaviors of flower-like MoS_2 nanostructures, J. Mater. Chem. A, 2 (2014) 15958–15963.
[22] H. Zhang, Ultrathin two-dimensional nanomaterials, ACS Nano, 9 (2015) 9451–9469.
[23] J. Chao, J. Deng, W. Zhou, J. Liu, R. Hu, L. Yang, M. Zhu, O.G. Schmidt, Hierarchical nanoflowers assembled from MoS_2/polyaniline sandwiched nanosheets for high-performance supercapacitors, Electrochim. Acta, 243 (2017).
[24] Y.H. Wang, K.J. Huang, X. Wu, Recent advances in transition-metal dichalcogenides based electrochemical biosensors: A review, Biosens. Bioelectron., 97 (2017) 305–316.
[25] S. Wang, L. Tan, P. Liang, T. Liu, J. Wang, C. Fu, J. Yu, J. Dou, H. Li, X. Meng, Layered MoS_2 nanoflowers for microwave thermal therapy, J. Mater. Chem. B, 4 (2016) 2133–2141.
[26] R. Sasikala, A.P. Gaikwad, O.D. Jayakumar, K.G. Girija, R. Rao, A.K. Tyagi, S.R. Bharadwaj, Nanohybrid MoS_2-PANI-CdS photocatalyst for hydrogen evolution from water, Colloids Surf., A, 481 (2015) 485–492.
[27] G. Yang, C. Chen, X. Tan, H. Xu, K. Zhu, Polyaniline-modified 3D-flower-like molybdenum disulfide composite for efficient adsorption/photocatalytic reduction of Cr(VI), J. Colloid Interface Sci., 476 (2016) 62–70.
[28] H.L. Shuai, K.J. Huang, Y.X. Chen, L.X. Fang, M.P. Jia, Au nanoparticles/hollow molybdenum disulfide microcubes based biosensor for microRNA-21 detection coupled with duplex-specific nuclease and enzyme signal amplification, Biosens. Bioelectron., 89 (2017) 989–997.
[29] H.L. Shuai, X. Wu, K.J. Huang, Molybdenum disulfide sphere-based electrochemical aptasensors for protein detection, J. Mater. Chem. B, 5 (2017).
[30] X. Zheng, J. Xu, K. Yan, H. Wang, Z. Wang, S. Yang, Space-confined growth of MoS_2 nanosheets within graphite: the layered hybrid of MoS_2 and graphene as an active catalyst for hydrogen evolution reaction, Chem. Mater., 26 (2014) 2344–2353.
[31] R. Tenne, M. Redlich, Recent progress in the research of inorganic fullerene-like nanoparticles and inorganic nanotubes, Chem. Soc. Rev., 39 (2010) 1423–1434.
[32] W. Zhou, D. Hou, Y. Sang, S. Yao, J. Zhou, G. Li, L. Li, H. Liu, S. Chen, MoO_2 nanobelts@nitrogen self-doped MoS_2 nanosheets as effective electrocatalysts for hydrogen evolution reaction, J. Mater. Chem. A, 2 (2014) 11358–11364.
[33] G. Ma, H. Peng, J. Mu, H. Huang, X. Zhou, Z. Lei, In situ intercalative polymerization of pyrrole in graphene analogue of MoS_2 as advanced electrode material in supercapacitor, J. Power Sources, 229 (2013) 72–78.
[34] L. Yang, S. Wang, J. Mao, J. Deng, Q. Gao, Y. Tang, O.G. Schmidt, Hierarchical MoS_2/polyaniline nanowires with excellent electrochemical performance for lithium-ion batteries, Adv. Mater., 25 (2013) 1180–1184.
[35] L. Hu, Y. Ren, H. Yang, Q. Xu, Fabrication of 3D hierarchical MoS_2/polyaniline and MoS_2/C architectures for lithium-ion battery applications, ACS Appl. Mat. Interfaces, 6 (2014) 14644–14652.
[36] Z. Liu, X. Wang, P. Qiao, Y. Tian, H. Li, J. Yang, Uniformed polyaniline supported MoS_2 nanorod: a photocatalytic hydrogen evolution and anti-bacteria material, J. Mater. Sci. Mater. Electron., 26 (2015) 7153–7158.
[37] T. Yang, H. Chen, T. Ge, J. Wang, W. Li, K. Jiao, Highly sensitive determination of chloramphenicol based on thin-layered MoS_2/polyaniline nanocomposite, Talanta, 144 (2015) 1324–1328.
[38] H.Y. Chen, J. Wang, L. Meng, T. Yang, K. Jiao, Thin-layered MoS_2/polyaniline nanocomposite for highly sensitive electrochemical detection of chloramphenicol, Chin. Chem. Lett., 27 (2016) 231–234.
[39] R. Yang, J. Zhao, M. Chen, Y. Tao, S. Luo, K. Jiao, Electrocatalytic determination of chloramphenicol based on molybdenum disulfide nanosheets and self-doped polyaniline, Talanta, 131 (2015) 619–623.
[40] J. Hui, X. Jiang, H. Xie, D. Chen, J. Shen, X. Sun, W. Han, J. Li, L. Wang, Laccase-catalyzed electrochemical fabrication of polyaniline/graphene oxide composite onto graphite felt electrode and its application in bioelectrochemical system, Electrochim. Acta, 190 (2016) 16–24.
[41] H. Xie, M. Yan, Q. Zhang, H. Qu, J. Kong, Hemin-based biomimetic synthesis of PANI@iron oxide and its adsorption of dyes, Desal. Water Treat., 67 (2017) 346–356.
[42] B.L. Li, H.Q. Luo, J.L. Lei, N.B. Li, Hemin-functionalized MoS_2 nanosheets: Enhanced peroxidase-like catalytic activity with a steady state in aqueous solution, Rsc Adv., 4 (2014) 24256–24262.
[43] M. Maqsood, S. Afzal, A. Shakoor, N.A. Niaz, A. Majid, N. Hassan, H. Kanwal, Electrochemical properties of PANI/MoS_2 nanosheet composite as an electrode materials, J. Mater. Sci. Mater. Electron., (2018) 1–8.
[44] K.J. Huang, J.Z. Zhang, Y.J. Liu, L.L. Wang, Novel electrochemical sensing platform based on molybdenum disulfide nanosheets-polyaniline composites and Au nanoparticles, Sens. Actuators B, 194 (2014) 303–310.
[45] S. Zhang, M. Zeng, W. Xu, J. Li, J. Li, J. Xu, X. Wang, Polyaniline nanorods dotted on graphene oxide nanosheets as a novel super adsorbent for Cr(VI), Dalton Trans., 42 (2013) 7854–7858.
[46] Z. Ying, H. Chen, L. Jie, C. Chen, Hierarchical MWCNTs/Fe_3O_4/PANI magnetic composite as adsorbent for methyl orange removal, J. Colloid Interface Sci., 450 (2015) 189–195.
[47] W. Wang, J. Tang, S. Zheng, X. Ma, J. Zhu, F. Li, J. Wang, Electrochemical determination of bisphenol A at multi-walled carbon nanotubes/poly (crystal violet) modified glassy carbon electrode, Food Anal. Methods, (2017) 1–10.
[48] H. Yin, Y. Zhou, Q. Ma, S. Ai, P. Ju, L. Zhu, L. Lu, Electrochemical oxidation behavior of guanine and adenine on graphene–Nafion composite film modified glassy carbon electrode and the simultaneous determination, Process Biochem., 45 (2010) 1707–1712.

[49] Han, Miao, Qu, Ying, Chen, Shiqin, Wang, Yali, Zhang, Zhi, Amperometric biosensor for bisphenol A based on a glassy carbon;electrode modified with a nanocomposite made from polylysine, single;walled carbon nanotubes and tyrosinase, Mikrochim. Acta, 180 (2013) 989–996.
[50] Y. Zhang, P. Chen, F. Wen, C. Huang, H. Wang, Construction of polyaniline/molybdenum sulfide nanocomposite: characterization and its electrocatalytic performance on nitrite, Ionics, 22 (2016) 1095–1102.
[51] T. Zhan, Y. Song, Z. Tan, W. Hou, Electrochemical bisphenol A sensor based on exfoliated Ni 2 Al-layered double hydroxide nanosheets modified electrode, Sens. Actuators, B, 238 (2017) 962–971.
[52] N. Ben Messaoud, M.E. Ghica, C. Dridi, M. Ben Ali, C.M.A. Brett, Electrochemical sensor based on multiwalled carbon nanotube and gold nanoparticle modified electrode for the sensitive detection of bisphenol A, Sens. Actuators, B, 253 (2017) 513–522.
[53] E.R. Santana, C.A.D. Lima, J.V. Piovesan, A. Spinelli, An original ferroferric oxide and gold nanoparticles-modified glassy carbon electrode for the determination of bisphenol A, Sens. Actuators, B, 240 (2017) 487–496.
[54] B. Su, H. Shao, N. Li, X. Chen, Z. Cai, X. Chen, A sensitive bisphenol A voltammetric sensor relying on AuPd nanoparticles/graphene composites modified glassy carbon electrode, Talanta, 166 (2017) 126–132.
[55] T. Zhan, S. Yang, X. Li, W. Hou, Electrochemical sensor for bisphenol A based on ionic liquid functionalized Zn-Al layered double hydroxide modified electrode, Mater. Sci. Eng., C, 64 (2016) 354–361.
[56] F. Tan, L. Cong, X. Li, Q. Zhao, H. Zhao, X. Quan, J. Chen, An electrochemical sensor based on molecularly imprinted polypyrrole/graphene quantum dots composite for detection of bisphenol A in water samples, Sens. Actuators, B, 233 (2016) 599–606.
[57] Y. Tan, J. Jin, S. Zhang, Z. Shi, J. Wang, J. Zhang, W. Pu, C. Yang, Electrochemical determination of bisphenol A using a molecularly imprinted chitosan-acetylene black composite film modified glassy carbon electrode, Electroanalysis, 28 (2016) 189–196.
[58] Y. Yang, H. Zhang, C. Huang, N. Jia, MWCNTs-PEI composites-based electrochemical sensor for sensitive detection of bisphenol A, Sens. Actuators, B, 235 (2016) 408–413.
[59] Y. Lin, K. Liu, C. Liu, Y. Lu, Q. Kang, L. Li, B. Li, Electrochemical sensing of bisphenol A based on polyglutamic acid/amino-functionalised carbon nanotubes nanocomposite, Electrochim. Acta, 133 (2014) 492–500.
[60] Y. Zhang, Y. Cheng, Y. Zhou, B. Li, W. Gu, X. Shi, Y. Xian, Electrochemical sensor for bisphenol A based on magnetic nanoparticles decorated reduced graphene oxide, Talanta, 107 (2013) 211–218.